

Modeling Seashell Morphology

George L. Ashline

Department of Mathematics
Saint Michael's College
Colchester, VT 05439
gashline@smcvt.edu

Joanna A. Ellis-Monaghan

Department of Mathematics
Saint Michael's College
Colchester, VT 05439
jellis-monaghan@smcvt.edu

Zsuzsanna M. Kadas

Department of Mathematics
Saint Michael's College
Colchester, VT 05439
zkadas@smcvt.edu

Declan J. McCabe

Department of Biology
Saint Michael's College
Colchester, VT 05439
dmccabe@smcvt.edu

June 23, 2009

Abstract

Modeling the beautiful and varied shapes of seashells sculpted by nature is an aesthetically appealing application of several concepts typically introduced in multivariable calculus. We use vector calculus tools to generate three-dimensional models of mollusk shells from growth measurements. We suggest a method for measuring shell specimens to determine necessary model parameters. We also provide Maple code for the modeling and several project handouts designed for various levels of student independence and preparation.

MATHEMATICAL FIELD: Calculus.

APPLICATION FIELDS: Malacology, paleontology, and marine biology.

TARGET AUDIENCE: Students in multivariable calculus.

PREREQUISITES: Multivariable calculus including space curves, parameterized surfaces, Frenet frames. Use of a computer algebra system for curve-fitting and generating three-dimensional graphics.

Contents

| | | |
|----------|---|-----------|
| 1 | Introduction | 5 |
| 2 | Developing the Model | 6 |
| 3 | Measuring the Shells and Fitting the Model | 9 |
| 4 | Parameter Effects and Surface Ornamentation | 13 |
| 5 | Project Handouts | 16 |
| 5.1 | Handout I (highly independent) | 16 |
| 5.2 | Handout II (breaking the problem into steps) | 17 |
| 5.3 | Handout III (structured format) | 17 |
| 5.4 | Handout IV (writing component) | 18 |
| 6 | Maple Code | 19 |
| 6.1 | Part I: the procedure “Shell” | 20 |
| 6.2 | Part II: modeling a shell specimen from data | 22 |
| 6.3 | Generating the color plate shells | 25 |
| 7 | References and Sources | 27 |
| 7.1 | Print shell modeling resources | 27 |
| 7.2 | Online shell modeling resources | 29 |
| 7.3 | Online sources for shells, pictures, and X-rays | 31 |

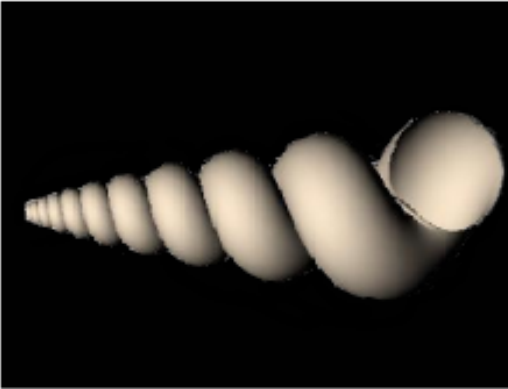


Plate 1.

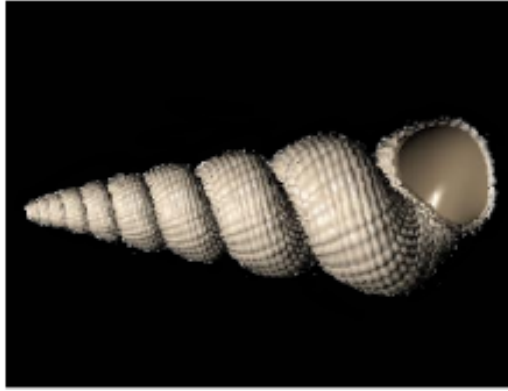


Plate 2.



Plate 3.

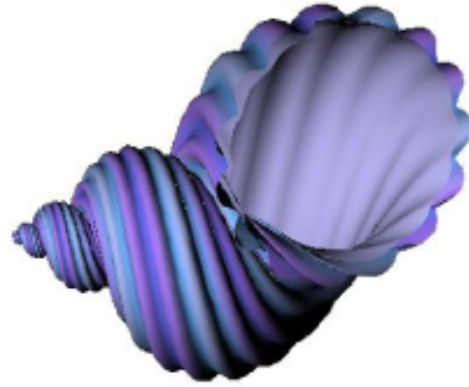


Plate 4.



Plate 5.

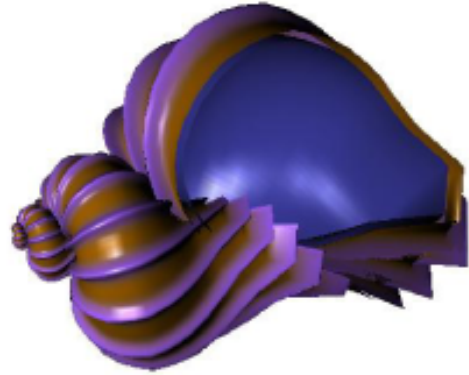


Plate 6.



Plate 7.

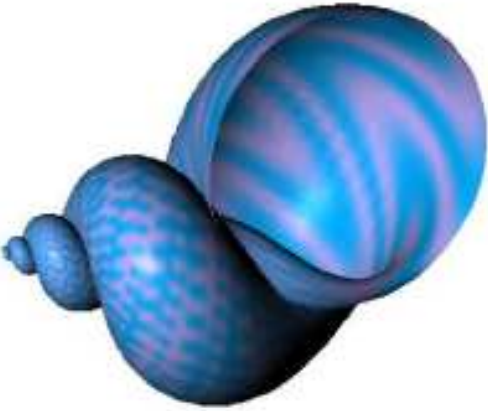


Plate 8.

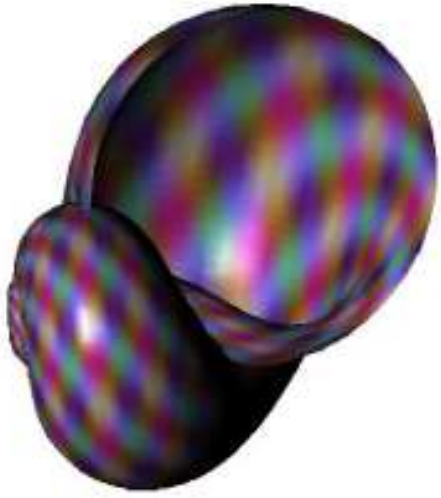


Plate 9.



Plate 10.

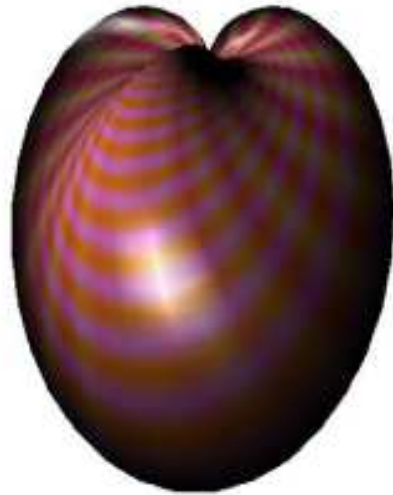


Plate 11.



Plate 12.

1 Introduction

The elegant shape of seashells has always attracted the eye of the artist, the scientist, and the mathematician. Despite the staggering variety of shell shapes found in nature, the growth of almost all seashells can be described in terms of three exponential functions and a closed curve that describes the shape of the shell's aperture, or opening. The model developed here is an aesthetically appealing application of several concepts typically introduced in multivariable calculus; it reinforces students' understanding of curves and surfaces in three-dimensional space, in particular, Frenet frames and parameterized surfaces. It also offers a taste of the challenges of collecting and using data in the modeling process. To model the morphology of specific shells, students take measurements from shell X-rays or photographs of cross-sections. They use these data to estimate several growth parameters that determine the overall three-dimensional shape of the shell. Curve-fitting is then used to more accurately model the aperture, enhancing the detail of the final model.

We focus on mollusks in the class *Gastropoda*. This class includes the familiar garden snails, slugs, and edible snails as well as a diverse array of freshwater and marine species, including periwinkles and whelks. Most shelled gastropods have a shell consisting of one piece, which is typically coiled or spiral in shape. Mollusks with one shell are referred to as univalves, while those with shells consisting of two parts, such as clams, mussels, and oysters, are called bivalves. Gastropods enlarge their helical shells by depositing fresh material at the lip of the aperture, or opening of the shell. The turns of the spiral of the shell are called *whorls*; the last-deposited and largest whorl of the shell is termed the *body whorl*, and the older, smaller whorls constitute the *spire* of the shell. Gastropod shells are composed largely of calcium carbonate overlaid by a tough protinaceous material called conchin or conchiolin. The protinaceous layer or periostracum imparts shell color in most cases [Rupert and Barnes 1994].

While the majority of shells have the asymmetrical helico-spiral shape described eloquently by D'Arcy Thompson (see Section 2), some shells such as the limpet are more symmetrical, and others like the cowrie shells are superficially bilaterally symmetric because each new whorl completely envelops previous whorls. We will work with the more typical helico-spiral shells, since their growth parameters may be more readily approximated.

From a strictly biological point of view, mathematical models of gastropod shells are of interest for several reasons. Extrapolations beyond the size of a particular shell can be constructed and viewed to determine whether the resulting shape retains its integrity or results in a loose spiral no longer connected to previous whorls. One can also determine if additional whorls would continue to increase the cross-sectional area of the aperture or if the aperture would be impinged upon by previous whorls, thus making the shell uninhabitable. This would indicate whether the particular growth parameters limit the range of sizes possible for a given species. The parameters can also aid in classifying the organisms by locating each species in a parameter space where each axis corresponds to one of the growth parameters. This helps to determine the spectrum of possible shell forms and may elucidate the relationship between different species [Raup 1966]. Finally, cross-sections of embedded fossils can

be measured and modeled to produce three-dimensional renderings without risking damage to valuable specimens.

In Section 2, we develop the parametric equations that model the surface of the shell. Section 3 describes the process of measuring a shell X-ray to determine the growth parameters and create a model of a particular specimen of *Epitonium magnificum*. The effects of varying the model parameters are discussed in Section 4, as are modifications to include surface ornamentation. Project handouts are included in Section 5. Section 6 provides Maple code for computing and plotting shell models; the process of modeling *E. magnificum* is included as a sample. Maple code for generating all of the color plates is also included here. The final section is an annotated list of references and resources for seashell modeling.

2 Developing the Model

The model we develop below is largely based on Prusinkiewicz and Fowler [2003], or Chapter 10 in Meinhardt [2003], particularly in the use of a Frenet frame to position the aperture. However, we loosely follow Jirapong and Krawczyk [2003] in taking measurements from a cross-section of the shell and using curve-fitting methods to fit exponential functions to the data. The underlying idea, captured by D'Arcy Thompson in his classic work *On Growth and Form*, is this:

The surface of any shell...may be imagined to be generated by the revolution about a fixed axis of a closed curve, which, remaining always geometrically similar to itself, increases its dimensions continually.... In turbinate shells, [any given point on the generating curve]... partakes, therefore, of the character of a helix, as well as a logarithmic spiral; it may be strictly entitled a helico-spiral [Thompson 1961, 189].

To visualize the growth of the seashell, we begin with a helical spiral rotating about the z -axis. Both the radius and the height increase as the animal grows, so the shell grows upwards along the z -axis, with the small end toward the origin, and the large open end further up the z -axis. The aperture is a closed curve that sweeps along this helical spiral, growing larger, but remaining geometrically self-similar as it moves along. See Figure 1, where we have flipped the image upside down to present a more typical view of the shell.

Seashell growth is in principle self-similar; the rate of change of both the radius and height of the helical spiral are proportional to their size, that is, both grow exponentially. Thus, if t is the angle of rotation about the z axis, the radius and height functions are given by:

$$\text{Radius: } r(t) = r_0 e^{k_r t};$$

$$\text{Vertical Displacement: } z(t) = z_0 e^{k_z t}.$$

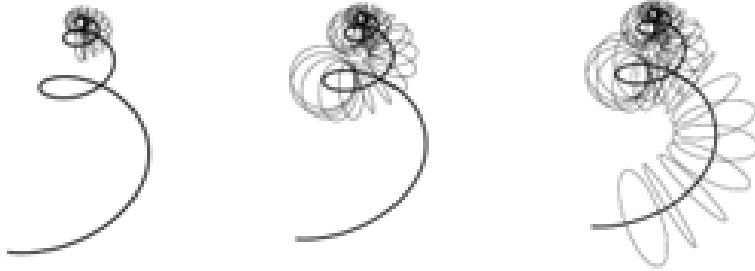


Figure 1: Growing circles sweep along the helical spiral to generate the shell surface.

Here k_r and k_z are the nonnegative growth constants. The constants r_0 and z_0 are initial radius and height values. The helical spiral is then given by the space curve:

$$H(t) = \langle r(t) \cos t, r(t) \sin t, z(t) \rangle.$$

Note that this helical spiral grows in the clockwise direction and thus produces a right-handed, or *dextral*, shell. This is by far the most common form, although a few genera normally produce *sinistral* shells, and rarely, a sinistral specimen of a normally dextral genus may occur [Oliver, 2004].

Just like the height and radius, the size of the aperture grows exponentially as the aperture sweeps along the helical spiral. We model the aperture as the product of an exponential growth function $a(t)$ and a ‘shape’ function $P(s)$. Here, as above, t is the angle of rotation about the z -axis. $P(s)$ is a polar function where s is a radial angle measured about the center of the aperture (a point on the helical spiral). Thus, the aperture is modeled by:

$$P(s) \cdot a(t), \text{ with } a(t) = a_0 e^{k_a t},$$

where k_a is the nonnegative growth rate and a_0 is the initial aperture size. If $P(s)$ is set equal to the constant 1, the aperture is simply a circle whose radius increases exponentially with t , as in Figure 1. It is easiest to begin by modeling a shell with a nearly circular aperture, or to use a circle as a first approximation of the aperture shape. When the rough overall form of the shell has been achieved, the aperture shape can be modified to give a more accurate image. The parameters r_0 , z_0 , a_0 , k_r , k_z and k_a for a particular gastropod may be estimated from measurements taken from the shell, as described in Section 3. The effects of varying these parameters are discussed in Section 4.

The shapes of shell apertures vary widely: some are nearly circular or elliptical, others nearly triangular, and still others quite irregular. Currently, there is no known elementary

function model for the aperture, as there is for the helical spiral. Thus, the aperture is typically approximated by using a variety of curve-fitting techniques, as discussed in Section 3.

It now remains to locate this aperture properly in space as the shell grows. The shell aperture lies in the plane perpendicular to the helical spiral at each point, that is, perpendicular to the tangent vector to the helical spiral space curve $H(t)$. Because of this, the model uses the Frenet frame of the helical spiral to position the aperture. The Frenet frame, also known as the TNB frame, consists of the unit tangent, normal and binormal vectors to a curve, here $H(t)$. We position the aperture in the the normal plane, which is perpendicular to the tangent vector and contains the normal and binormal vectors, as shown in Figure 2. This controls the tilt of the shell opening to give a life-like result. Without the Frenet frame, the shell opening and any ridges would always be parallel with the z -axis, thus inaccurately modeling the shell morphology [Prusinkiewicz and Fowler 2003].

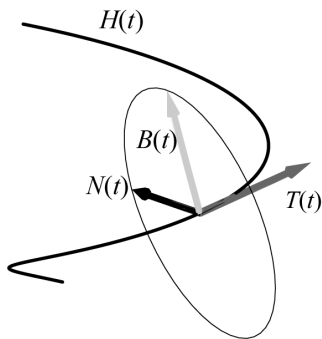


Figure 2: Circular shell aperture lying in the plane normal to $H(t)$.

To find the unit normal and binormal vectors, respectively $N(t)$ and $B(t)$, of the helical spiral $H(t)$ at a given t , first find its unit tangent vector

$$T(t) = H'(t)/|H'(t)|.$$

Next,

$$N(t) = \frac{T'(t)}{|T'(t)|},$$

and

$$B(t) = T(t) \times N(t).$$

The surface S of the shell is then modeled by:

$$S(s, t) = H(t) + P(s) \cdot a(t) (\cos(s)N(t) + \sin(s)B(t)),$$

where $0 \leq s \leq 2\pi$ and, generally, $t \geq 0$.

The equation for the two-parameter surface $S(s, t)$ makes it easy to visualize how the surface is traced out: for each value of t , the tip of the vector $H(t)$ is a point on the helical spiral; the second term is a radial vector that traces the aperture curve centered at that point in the normal plane. See Figure 3.

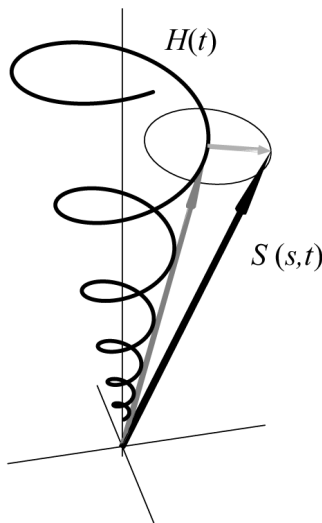


Figure 3: The shell surface traced out as the sum of two vectors.

Ultimately, six parameters and one function are used in this equation for modeling shell morphology: the initial value parameters r_0, z_0, a_0 and the growth parameters k_r, k_z, k_a for the exponential functions that fit the shell measurements, together with the radial aperture shape function $P(s)$. By adjusting the parameters that control the helical spiral and aperture growth and specifying $P(s)$, a large variety of naturally occurring shells can be modeled and fantasy shells can be created as well.

3 Measuring the Shells and Fitting the Model

This section gives explicit directions for measuring shell specimens to determine the necessary model parameters $r_0, z_0, a_0, k_r, k_z, k_a$ and to approximate $P(s)$. It is possible to work directly from an actual seashell to obtain the parameters, either by taking external incremental caliper measurements or by cutting the shell lengthwise through its axis in order to reveal the interior structure. Both of these methods have been used by prior modelers [Jirapong and Krawczyk 2003, Prusinkiewicz and Fowler 2003], but both require access to the actual shell. To simplify the process, we chose to work with X-ray images of shells available for purchase [Crow 2009], and we used a hard copy of a shell image large enough to be easily measured with a ruler (about 15 centimeters tall works well). The measuring and fitting process is illustrated in Figures 4 and 5 for *E. magnificum*, a shell with nearly circular apertures. The Maple code in Section 6 carries out the calculations and renders the final image.

We begin by drawing the (vertical) axis through the image of the shell and choosing the point that will be designated the “apex” or tip of the shell. It is impossible to locate the apex definitively, and in some cases the true apex has been worn away, so we simply approximate as best we can. The variable t is set to zero at this point, and it increases by 2π each time the aperture completes a rotation about the axis, thus creating another whorl of the shell. Our model is “upside down” from the way shell images are typically depicted; this is because we think of our shells as growing upward from the origin. When we display the images, we typically rotate them to put the apex at the top again, as in Figure 1 and the color plates.

To determine the parameters k_r and k_z , we first need to locate the center of each of the cross-sectional apertures. Strictly speaking, the shell has only one aperture, the actual opening, but the cross-sections of the shell chamber visible in the X-ray image were the apertures at some times in the past as the shell was growing, so we refer to these cross-sections as apertures as well. Caution is needed in taking measurements of the smallest few apertures. Not only are the apical whorls of the shell hard to measure due to their size, but they were laid down by the animal in its larval stage and are typically structurally different from the rest of the shell. Furthermore, when modeling a cut shell, the chambers near the apex may be distorted as the cut is often somewhat off-center. Finally, at the opposite end of the shell, the actual opening of the body whorl of the shell may deviate from the shape of the other cross-sections, so, if possible, it is best not to use it for measurements either. There should be at least 4 feasible cross-sections, using the actual opening and the apex chambers only as a last resort.

The whorl cross-sections correspond to t values that are integer multiples of π ; even multiples for sections on one side of the axis, odd for those on the other. For the model of *E. magnificum*, we choose 5 cross-sections to use for our calculations and denote these t values as t_i , for $i = 1, 2, \dots, 5$. See Figure 4. Using a ruler held parallel and then perpendicular to the shell axis, we draw rectangles circumscribed about each aperture, and locate the center, C_i , of each rectangle using diagonal intersections (if the apertures are circular, these should be their centers.) The points C_i are used to determine the path of the helical spiral that acts as the frame of the shell, and thus specify the growth functions $r(t)$ and $z(t)$.

We draw horizontal line segments from each center C_i to the shell axis; these lengths are denoted r_i . Next, we measure the vertical distance along the axis from the apex to the midpoint of each rectangle; these height measurements are denoted z_i . These data are given in Table 1. We then fit an exponential curve to the ordered pairs (t_i, r_i) to find the function $r(t)$; another exponential is fitted to (t_i, z_i) to find $z(t)$. This is done using the command `ExponentialFit` in Maple’s Statistics package to determine the parameters r_0 , k_r , and z_0 , k_z . The helical spiral can now be plotted.

To determine $a(t)$, the aperture growth function, we measure the half-heights of the rectangles; these are denoted h_i , and also given in Table 1. With the pairs (t_i, h_i) , we again use the Statistics package to find the parameters a_0 and k_a that give the best fit for the exponential function $a(t)$. Note that even if the apertures are circular, it is likely that $r_i \neq h_i$ because the apertures are generally not tangent to the shell axis. The coiling shell forms a cone-shaped structure, the *columella*, running along the axis of the shell, and

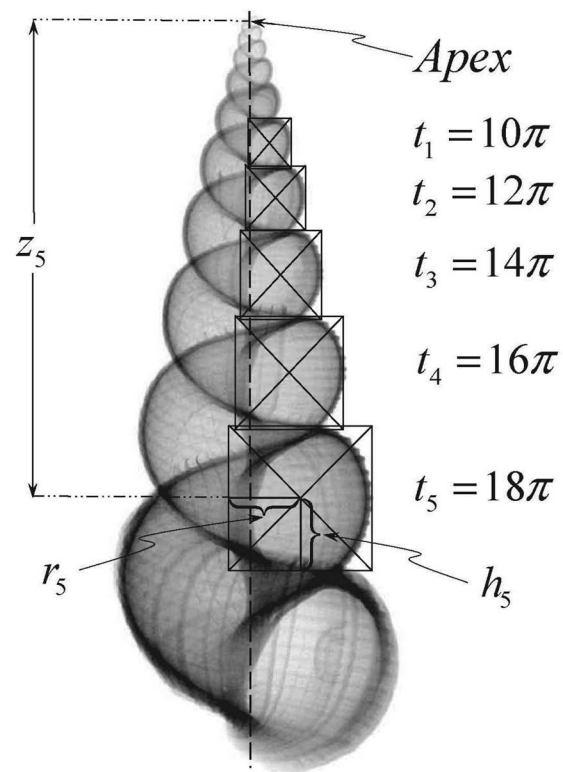


Figure 4: Measuring the radii, heights, and aperture heights from an X-ray of *E. magnificum* (not to scale).

Table 1: Growth parameter measurements for *E. magnificentum*, with θ in radians, and r_i , z_i , and h_i in cm.

| | θ | r_i | z_i | h_i |
|---|----------|-------|-------|-------|
| 1 | 10π | 0.4 | 2.5 | 0.55 |
| 2 | 12π | 0.5 | 3.6 | 0.65 |
| 3 | 14π | 0.6 | 5.1 | 0.85 |
| 4 | 16π | 0.8 | 7.0 | 1.15 |
| 5 | 18π | 1.0 | 9.7 | 1.50 |

the apertures connect to it. This cone, which may be solid or hollow, forms the structural support of the shell, and the gastropod’s foot is attached to it by means of the columella muscle, which retracts the entire animal into the shell [Jirapong and Krawczyk 2003; Rupert and Barnes 1994]. A model of the shell with circular apertures can now be plotted. See Color Plate 1.

For *E. magnificentum*, the likeness is quite good, and the model represents the shape and dimensions accurately. Notice, however, that the apertures on the X-ray image are not perfectly circular. Proceeding on the widely accepted assumption that whorl cross-sections are all geometrically similar, we choose one of the apertures (in this case, the one at $t = 18\pi$) and approximate as best we can the radial shape function $P(s)$. One difficulty is that in an X-ray or cross-section of the shell, the displayed openings are all in a plane parallel to the z -axis, and thus are not actually in the plane of the aperture. However, for most shells, the ‘tilt’ toward the tangent vector is small enough that we can still get a reasonable approximation of the aperture shape from the available cross-section. Apertures vary widely, and there are no rules to guide us about what form to use for the radial function; insight and ingenuity are encouraged in this process.

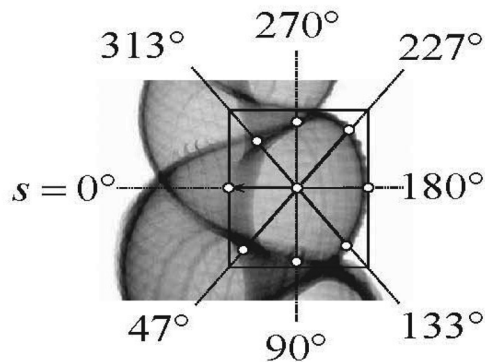


Figure 5: Radial measurements for the aperture, with the polar axis indicated by an arrow-head (not to scale).

Table 2: Radial measurements for aperture $P(s)$.

| s (degrees) | radius (cm) |
|---------------|-------------|
| 0 | 0.52 |
| 47 | 0.58 |
| 90 | 0.54 |
| 133 | 0.60 |
| 180 | 0.54 |
| 227 | 0.60 |
| 270 | 0.52 |
| 313 | 0.46 |
| 360 | 0.52 |

We begin by taking some radial measurements using a protractor and ruler, as shown in Figure 5 and given in Table 2. We align the polar axis at $s = 0$ with the normal vector, and measure counterclockwise from there. This orients the aperture appropriately with the way the surface is traced by $S(s, t)$. Figure 5 shows the polar axis as horizontal, even though the normal vector is actually tilted slightly off the horizontal. Nevertheless, this approximation gives acceptable results.

The number of measurements needed to produce a realistic rendering depends on the aperture shape: based on our experience, if the aperture is fairly smooth and roughly circular, 6 or 8 points might suffice, while if it is irregular, many more points may be needed. Plotting these measurements as functions of the central angle s may suggest a form for $P(s)$. For some shells, a sinusoidal curve might produce an appropriate ribbed effect. The first few terms of a Fourier series may produce a better fit, or a polynomial function of an appropriate degree might work. Curve-fitting packages provide the option of choosing any of these forms to be fitted, as long as the function parameters appear linearly. However, a piece-wise linear or spline approximation may be needed for a good fit. Maple’s “Interactive” curve-fitting feature can be a quick and useful tool for this part of the modeling. For *E. magnificum*, we use a Fourier sum with terms up to $\sin(3s)$ and $\cos(3s)$. The shape of the aperture may be seen in the $x - y$ plane by plotting $P(s) \cdot \langle \cos(s), \sin(s) \rangle$. Once $P(s)$ is determined, we have all the information necessary to create a life-like three-dimensional model of the shell, shown in Color Plate 2. This rendering is very close to the actual shell shown in Color Plate 3.

4 Parameter Effects and Surface Ornamentation

Whether attempting to model an actual shell specimen or creating seashell shapes purely for pleasure, it is important to understand how the various parameters affect the shape of the shell, and how to achieve some of the common surface ornamentations such as ribs and ridges. We have found that creating fantasy shells is not only a lot of fun and artistically

appealing, but also develops a sense of the parameter interactions. Color Plates 4 through 12 show “designer shells” that have been created to illustrate various parameter interactions, apertures, and surface orientation.

The helico-spiral $H(t)$ described in Section 2 provides the structural frame for the shell. The radial and vertical growth parameters k_r and k_z , and, more specifically, their ratio, determines the shape of the helical spiral *envelope* (the curve through the points where the spiral intersects the first quadrant of the $x - z$ plane) and hence the overall silhouette of the shell. If $k_r = k_z$, then the envelope will just be a straight line, as in Figure 6, and the result is usually a conical shell, as in Color Plate 8.

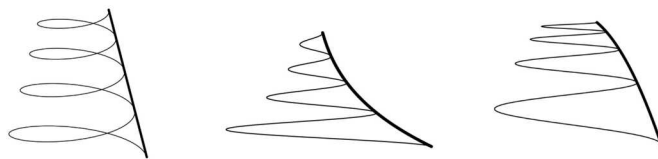


Figure 6: Envelope of the helico spiral: linear (left), pointy shell (center), flattop shell (right).

More generally, if $k_r \cdot k_z \neq 0$, then the envelope is a power function, with z as a function of r , as follows. Solving the radial equation $r = r_0 e^{k_r t}$ for t , we obtain $t = (1/k_r) \ln(r/r_0)$. Substituting this into $z = z_0 e^{k_z t}$, we find that $z = z_0 e^{(k_z/k_r) \ln(r/r_0)} = z_0 e^{\ln((r/r_0)^{(k_z/k_r)})}$, and hence

$$z = \left(\frac{z_0}{r_0^{k_z/k_r}} \right) r^{k_z/k_r}. \quad (1)$$

Thus, the ratio of k_z to k_r determines whether the shell will have a pointy top or a flat top, as illustrated in Figure 6. From equation 1, we see that if k_r is the greater, we have a shell with a pointy tip as in Color Plate 7, and if k_r is the lesser, we have a flat-tipped shell, as in Color Plate 9.

Note that the ratio of r_0 to z_0 scales the power function in Equation 1, so that, for example when $k_r = k_z$, this ratio controls the slope of the envelope of the helical spiral cone. More generally, the parameters r_0 and z_0 determine how vertically stretched out a shell appears. However, as discussed below, other factors also influence the final silhouette.

Another important factor affecting shell shape is the aperture growth function $a(t)$. The magnitude of the growth constant k_a will determine how “tightly packed” the shell whorls appear. If k_a is too small with respect to k_r , the shell forms a loose tube-like spiral; if k_a is too large, it “swallows up” previous whorls. This is illustrated by comparing Color Plates 10 and 12 to Color Plate 8. The shape of the aperture also contributes to the shell’s silhouette: two shells with the same helico-spiral $H(t)$ but different aperture shapes, say a circle and a triangle, would exhibit significantly different morphologies. Examining some shells with different cross-sections should make this clear. It might also be an interesting exercise to construct such shells for comparison.

Shells exhibit surface sculpting of many different types, described by terms such as ribs, grooves, cords, granules, nodules and scales [Egerton 2008]. Spiral and axial ribs are the most basic of these. *Spiral ribs* run parallel to the helico-spiral $H(t)$. Adding a periodic function in s , such as a sine function of appropriate period and amplitude, to an aperture function will create spiral ribs. *Axial ribs*, or *ridges*, are orthogonal to $H(t)$. On first glance, it may seem that ridges are vertical, that is, parallel to the z axis. But closer examination of shell specimens shows that ridges occurring in nature, in fact, lie in planes perpendicular to the helico-spiral $H(t)$ [Prusinkiewicz and Fowler 2003]. Some of these ridges are, actually varices, thickenings that result from pauses in the growth of the shell, so they must lie in the aperture plane [Oliver and Nicholls 2004]. This confirms that the Frenet frame is the appropriate method for modeling shells, and it allows ridges to be incorporated in a straightforward way. In modeling the shell exterior, ridges may be regarded as periodic (or at least recurrent) changes in the aperture. Ridges can thus be incorporated by modifying the shape function so that it varies with t as well as s . Letting $\hat{P}(s, t) = P(s) \cdot Q(t)$, with the variables separated, keeps the aperture shape geometrically similar along the length of the helico-spiral, but allows t -variations that may create ridges. Allowing P to be a more general function of s and t would permit aperture shape to vary in all sorts of ways and not remain geometrically self-similar. Shells with ribs and ridges are illustrated in Color Plates 4, 5, and 6.

Some shells have highly convoluted apertures that may simply not be expressible as a polar function. Other methods for defining the generating curve, such as Bézier curves, have been used [Prusinkiewicz and Fowler 2003], but these are beyond the scope of our two-parameter model.

Despite careful measuring, the resulting models often differ somewhat from the chosen specimen. One source of error we have noticed is that the model can be quite sensitive to the initial values r_0 and z_0 . The helical spiral might seem to have the correct proportions based on the measurements, but the final shell appears too elongated or too squat. In that case, some minor *ad hoc* adjustments may be necessary to achieve a good rendering. Another difficulty is that, for both shell X-rays and cross-sections of actual shells, the visible cross-sections lie in a plane containing the z -axis, not in a plane determined by the Frenet frame, so the aperture curve derived from measurements is distorted. A nice extra-credit problem is to adjust the measurements for distortion by taking into account how far the Frenet frame is tilted away from the vertical. A third caution is that some shells with elongated apertures (*Cymantium Clandestina* for example) may have have a small narrow portion of the aperture that does not lie in the normal plane, but rather inclines toward the z -axis.

We initially estimated designer shell parameters from photographs, but then also gave free rein to artistic license. Our color patterns result from specifying *RGB* colors as functions of s and t in our Maple plots. Although it is fun to play with the color patterns this way, it generally does not replicate actual shell coloration (except stripes). See Meinhardt [2003] for further information, and stay tuned for a seashell patterning sequel to this module! Bivalves (such as clams or cockles) may also be modeled using the methods shown here, as in Color Plates 11 and 5, but we have not yet found a satisfactory way to estimate the parameters from shell measurements. However, eyeball estimates and a good understanding of how

the parameters control the shape of the shell can still lead to lovely renderings. The shell parameters and aperture functions used to generate the designer shells in Color Plates 4 through 12 are given in Section 6.3

5 Project Handouts

The handouts below offer several possible approaches for this project, ranging from highly independent to quite structured. For an independent approach, we provide Handout I only. For classes or students needing more guidance, we also provide Handout II, which breaks down the problem into smaller steps. Handout III further assists students with organizing their work. We have successfully used the Handout I only approach in class and were gratified by the enthusiasm with which students grappled with the problem. They were very excited by having an open-ended application and not being led by the hand through it. We encourage such independent students to share model drafts with us, if they wish to check their progress. However, as project work continues, some students need suggestions for breaking down the steps and we then provide Handout II to them. Handout III can help streamline assessment, particularly with less prepared students. Handout IV adds a writing component to the project.

Developing the model itself can be a valuable experience for well-prepared, self-motivated students. In this case, we provide students only with Handout I and part of the resource list from Section 7. We require students to gain morphology and modeling information directly from the literature without the benefit of the discussions contained in this module. By including Handout IV, we give students an opportunity to develop mathematical writing skills and more closely replicate a real-world experience in applied mathematics. Students completing a literature search can explore the range of works on this topic and may well improve on the model presented in this module.

In our courses, we begin this project after students have learned about space curves and Frenet frames. To facilitate the shell modeling, we introduce parameterized surfaces earlier than our textbook. We also loosely describe how a shell model is formed by the aperture curve sliding along the helical spiral, but mostly leave students to the satisfaction of independent discovery.

5.1 Handout I (highly independent)

Choose a seashell, either an intact shell or some form of cross-section, and develop the equations to model it. Write a program with course software to generate a three-dimensional model of the shell. The code must be well-documented (i.e. contain detailed explanations describing each line of code). In addition, demonstrate your understanding of how the various parameters in your model control shell morphology in a brief written explanation.

5.2 Handout II (breaking the problem into steps)

1. Choose an actual shell to model. You need to pick a shell where you can get a good picture of a cross-section of the inside of the shell. For example, you may use a shell X-ray or cross-section photo obtained from a text or reputable website.
2. Measure the shell to get the parameters necessary to write the equation for the helical spiral going through the center of the shell. You will need to take measurements at the same location in every opening on one side of your shell (or both sides if there are few openings). Use course software to fit a curve to these data, estimating the growth rates of the height and radius. Use this information to determine an equation for the helical spiral. Plot the helical spiral using course software.
3. Compute the Frenet frame at some convenient point on the space curve. Use course software to plot the curve together with the TNB vectors at the point.
4. Find the normal plane at the same point, and use course software to plot that plane with the space curve.
5. Find the equation of a circle with center at that point and lying in the normal plane, and plot it with the space curve.
6. Plot several circles of diminishing size up the helical spiral, with each circle lying in the Frenet frame at its center.
7. Assume the aperture is a circle with radius equal to the radius of the helical spiral at each point, and plot the resulting shell.
8. At this point, experiment with different aperture and growth functions to create and plot several fantasy shells. Explore the impact of changing the growth rates of the helical spiral's radius and/or height, or modifying the initial values of the radius and/or height.
9. Returning to your actual shell, measure 8 to 24 radial points, more if needed, on the aperture, and fit a curve to these points using a curve-fitting tool from course software.
10. Create a three-dimensional model of your shell.

5.3 Handout III (structured format)

Submit the following work showing how you developed a model for your shell:

1. An unmarked copy of the X-ray or cross-section photo of the shell you are modeling, with the source of the picture and the name of the shell. If possible, provide a photo of an intact shell of the same species.

2. A carefully marked copy of the X-ray or photo, indicating the measurements you took to determine the helical spiral parameters.
3. A table of the helical spiral and aperture growth parameter measurements.
4. Carefully documented work showing how you derived the helical spiral.
5. Work showing how you computed the Frenet frame, normal plane, and a circle in the normal plane at some point on the helical spiral.
6. Four printouts of the helical spiral, one with the Frenet frame, one with the normal plane, one with the single circle, and one with several circles of increasing size.
7. A plot of a shell with a circular aperture.
8. A carefully marked picture of the actual shell aperture, indicating the measurements you took for the curve-fitting.
9. A printout of the curve used to model the aperture.
10. Your carefully documented code.
11. A plot of a three-dimensional model of your shell.
12. At least one “fantasy shell,” developed from aesthetic principles.

5.4 Handout IV (writing component)

An important component of doing mathematics is developing the ability to learn new ideas independently by using texts, journal articles, and colleagues. This project is designed to give you some experience with the real thing.

Use both print and electronic resources to research and understand as much as you can about how to model shell shapes, and then write it up as clearly as possible. The mathematics is within your reach, but it will likely require translating notation and ideas into familiar notation and concepts from class. This will be true of almost any scientific application you encounter outside of the classroom. Also, many sources will not provide all of the details that you will need for your model, so you may have to fill in and figure out a lot on your own. Some sources may not measure the same shell features as others. Some modeling techniques may work better than others. Again, all of this is typical of material written for a particular scientific application, rather than for classroom use. A major goal of this project is to provide exposure to this reality and allow you to develop skills for using your course work in other endeavors.

Formatting guidelines

1. Include a title page and abstract.

2. Use a mathematical typesetting tool such as LaTeX or MathType for all equations and symbols, and prepare all figures carefully.
3. The paper must be properly referenced, with a complete bibliography at the end and references in the text. Internet resources must be used with caution and must be properly documented. Use MathSciNet <http://www.ams.org/mathscinet> as much as possible for citation formats. Use MLA formatting for Internet sites <http://www.wisc.edu/writing/Handbook/elecmla.html>, and for anything not on MathSciNet.
4. Model your paper on articles you read in your research, and consider both their structure and their content.
5. Proofread carefully. Use campus writing resources and peer review, and appropriately edit/revise your paper before submission.

Evaluation criteria

The overall goal is a clear model describing what measurements are needed from the shell, a formula for generating the shell, and a description of the effect of each variable in the formula. Clarity of exposition is as important as the underlying mathematics. Indications of a well-written paper: clear equations with careful discussions of which physical properties of the shell are controlled by which parameters, figures that illustrate the concepts you are discussing, and clear evidence that you understand basic vector calculus concepts and how they pertain to this application.

Indications of a paper that needs more work: equations and/or figures copied with inadequate explanation, disorganized composition, poor spelling or grammar, lack of proofreading, over-reliance on Internet sources, and inadequate referencing.

6 Maple Code

This project assumes a reasonable amount of familiarity with a computer algebra system that generates three-dimensional graphics. We use Maple throughout our calculus curriculum, so our students are familiar with basic function manipulation, plotting commands, and syntax when starting this project. As part of normal multivariable calculus class work, we also provide examples in Maple of generating space curves, parameterized surfaces, planes, and the Frenet frame, so this project also offers excellent synthesis and application opportunities.

Below is the Maple 12 code that we developed for this project. The generic Maple procedure, which may be used with any shell parameters, is provided first, followed by a sample of modeling a shell of the species *E. magnificum*. We do not necessarily expect students to be familiar with the procedure (proc) command used in the worksheet. Some students use it (particularly those with some computer science background), while others are more comfortable generating each shell plot individually. Both approaches seem to work equally well.

This worksheet has two parts. Part I is the procedure “Shell” that creates the plot of the shell model. Using the inputs given in Section 6.3, this procedure will generate all the images shown in the color plates. Part II is a sample of the modeling process for *E. magnificum*, using the shell measurements given in Tables 1 and 2 to estimate the growth parameters and model the shape of the aperture.

6.1 Part I: the procedure “Shell”

Using as input the growth parameters and the radial aperture function P , the procedure produces a plot of the three-dimensional shell model, as well as the helico-spiral, the envelope, and the aperture.

Parameters passed to the procedure:

- r_0, z_0, a_0 : values of the radius, height, and aperture size at $t = 0$;
- k_r, k_z, k_a : the radial, height, and aperture growth rate parameters, respectively;
- P : the aperture curve, a polar radius function of the angle s around the helical spiral, entered as a Maple expression. Note that if P is constant, the aperture is circular. Also, to create ribbed shells, we allow P to vary with t as well as s without changing the notation. (In the text, we use the notation $P(s, t)$).
- $tstart, tend$: the range of the angle of rotation about the z -axis;
- n, m : the number of points in the $n \times m$ grid used in generating the surface plot;
- R, G, B : color settings for the ambient light;
- l_1, l_2 : direction for the ambient light;
- cR, cG, cB : color settings for the shell – if these are expressions in s and t , they create the color patterns on the shells;
- $phi, theta$: set the viewing angle;
- $STyle$: the rendering style of the plot (one of: contour, hidden, line, patch, patchcontour, patchngrid, point, or wireframe).

Output variables for the procedure:

- $shellplot$: a plot of the three-dimensional shell rendering;
- $helix$: three-dimensional plot of the helico-spiral $H(t)$;
- $aptrace$: a two-dimensional plot of the aperture shape function;

- *envelope*: a plot of the envelope of $H(t)$ in three-dimensional space, which is a curve in the $x - z$ plane.

Note that procedures must be executed within a single execution group in Maple. The output from a procedure is usually in the form of a list, *ReturnVal*, found at the end of the procedure. Recall that, if L is a list, then $L[i]$ returns the i^{th} entry in the list, and this is how we choose from the list of plot structures output by the procedure.

```

>restart: with(plots):
>Shell:=proc(r0,z0,a0,Kr,Kz,Ka,P,tstart,tend,n,m,l1,l2,R,G,B,cR,
    cG,cB,phi,theta,STyle)
local r,H,FrenFrame,NormalVec,BinormalVec,Apert,shell,helix,
    aptrace,envelope,shellplot:
global S:
uses VectorCalculus,plots:
r:=t->r0*exp(Kr*t):
H:= t-> <r(t)*cos(t),r(t)*sin(t),z0*exp(Kz*t)>:
    helix := spacecurve([H(t)[1], H(t)[2], H(t)[3]], t=tstart..
        tend,numpoints=1000,color = red,orientation=[phi,theta],
        scaling = constrained):
    envelope:=spacecurve([v,0,z0*(v/r0)\symbol{94}(Kz/Kr)], v=r(
        tstart)..r(tend)):
    aptrace := spacecurve([P*cos(s),0,P*sin(s)],s=0..2*Pi,
        numpoints = 1000, orientation = [90, -90], scaling=
        constrained):
    FrenFrame := TNBFrame(H(t),t):
    NormalVec := FrenFrame[2]:
    BinormalVec := FrenFrame[3]:
    Apert := a0*exp(Ka*t)*P:
    shell := H(t)+NormalVec*Apert*cos(s)+BinormalVec*Apert*sin(s):
    shellplot := plot3d([shell[1],shell[2],shell[3]],t= tstart..tend
        ,s=0..2*Pi,orientation=[phi, theta],scaling = constrained,
        grid=[n,m],style=STyle, light=[l1, l2, R, G, B], color = [cR,
        cG, cB]):
    S := [shellplot,helix,aptrace,envelope]:
end proc:

```

Here is an example of displaying output from the procedure; the “display” command is used to exhibit two or more of the plots together.

```

>Shell(.1, 1.9, .2, 0.05, 0.04, 0.05, 1-0.08*sin(15*s), -6*Pi,
    6*Pi, 100,100, 0,0,.9, 1/2, .9, sin(10*s), 1, sin(5*s), -116,
    -90, patchnogrid):
>S[1]; S[2]; S[3];
>display({S[2],S[4]});

```

6.2 Part II: modeling a shell specimen from data

We model the X-ray image of *E. magnificum* [Crow 2009]. The modeling proceeds in two stages. First, we use shell measurements in Table 1 to estimate the growth parameters and create a model with a circular aperture. Then we use the radial aperture measurements in Table 2 to approximate the aperture shape more accurately.

Fitting exponential functions to data gathered from X-ray image measurements

Based on the shell specimen, we decide how many whorls of the shell to use to determine the growth constants k_r, k_z, k_a . In our shell image, five cross-sections at $t = 10\pi, \dots, 18\pi$ are used, as illustrated in Figure 4. Recall that t is the angle of rotation about the z -axis. The choice of where to set $t = 0$ is an “eyeball” estimate since the tip of the shell is anomalous. We create vectors of the t values and the corresponding r measurements:

```
>with(Statistics): with(VectorCalculus):  
>tvec:=evalf(< 10*Pi, 12*Pi, 14*Pi, 16*Pi, 18*Pi >):
```

We fit measurements of the helical radii r from Table 1 to the exponential function $r = r_0 e^{k_r t}$:

```
>rvec:= <0.4, 0.5, 0.6, 0.8, 1.0 >:  
>rparam:=ExponentialFit(tvec, rvec, t, output=parametervalues);  
>r0:=exp(rparam[1]); Kr:=rparam[2];
```

We use measurements of the helical heights z from Table 1, and again fit the data to the exponential function $z = z_0 e^{k_z t}$:

```
>zvec:= < 2.5, 3.6, 5.1, 7.0, 9.7 >:  
>ExponentialFit(tvec, zvec, t);  
>zparam:= ExponentialFit(tvec, zvec, t, output=parametervalues);  
> z0:=exp(zparam[1]); Kz:=zparam[2];
```

At this point, one could plot the helico-spiral to check whether measurements appear accurate and produce a suitable spiral.

The next step is to model the aperture. We begin by using a circle centered on the helico-spiral $H(t)$ with its radius increasing as it travels up the spiral.

To determine the constants for the aperture growth function $A(t)$, we use the measured “half-height” of the circumscribed rectangles, as shown in Figure 4. Once more, we fit the data given in Table 1 to an exponential function.

```
>hvec:= < 0.55, 0.65, 0.85, 1.15, 1.50 >:  
>ExponentialFit(tvec, hvec, t);  
>hparam:= ExponentialFit(tvec, hvec, t, output=parametervalues);
```

The parameter a_0 is the “initial” size of the aperture/cross-section, and k_a is the aperture growth constant:

```
>a0:= exp(hparam[1]); Ka:= hparam[2];
```

Shell model with circular aperture

We can now plot a model of the shell with circular apertures using the “Shell” procedure and the growth parameters we have determined.

Using $P = 1$ produces a circular aperture with size corresponding to the measurements taken.

```
>Shell(r0,z0,a0, Kr,Kz,Ka, 1, 0,20*Pi, 500,50, 60,0, 1,1,1,
      0.98,0.9,0.8, -90, -80, patchnograd):
>S[1];
```

To see an image that resembles the X-ray, right click and view the shell without the wireframe and with transparency adjusted to about 50%. Displaying the shell with SType set to wireframe helps determine the appropriate ratio of n to m in the grid setting. Adjust n and m so that the wireframe cells on the shell surface are roughly square.

Also, the shell grows with increasing z , so the graph has been turned upside down (using viewing angles phi and theta) to get the usual view.

Detailed aperture shape: curve-fitting for radial aperture function

We use radial measurements of the aperture at a fixed value of t to approximate the function $P(s)$. This section is intended as a sample only. Ingenuity is required when attempting to model shells with apertures that deviate significantly from a circle. As shown in Figure 5, we use the aperture at $t = 18\pi$, measuring radially at 8 locations ($s = 0, 47, 90, 133, 180, 227, 270, 313$ degrees) using a protractor. We use only the quadrantal angles and the diagonals of the rectangles; more data points are needed if the aperture shape is more irregular. The measurement data are given in Table 2.

```
>with(CurveFitting):
>anglvec:= evalf(Pi/180*< 0,47,90,133,180,227,270,313,360 >);
>with(plots):
>radvec:=<1.35, 1.6, 1.4, 1.4, 1.4, 1.5, 1.6, 1.2, 1.35>;
>pts:= seq([anglvec[i], radvec[i]], i=1..9);
>Points:=pointplot([pts], scaling=constrained):
>display(Points);
```

We want to fit a curve to these points on the interval $[0, 2\pi]$. There are many possibilities for the curve to be used, and a polynomial fit is certainly one options. When fitting to polynomials, going more than “once around” when fitting the curve may give a smoother result; this can be done automatically using the wrap feaure in the interactive fitting assistant. However, since the radial function is periodic, it seems natural to use a Fourier approximation. We use terms up to $\sin(3s)$ and $\cos(3s)$. After experimentation with more and fewer terms, this choice appears optimal since more terms don’t improve the fit and introduce undesirable “wiggles.”

```

>FourierForm:= k+a*sin(s) + b*cos(s) +c*sin(2*s) +d*cos(2*s)+e*
sin(3*s) +f*cos(3*s):
>ApFit:=LeastSquares(anglvec, radvec, s, curve=FourierForm);
>FitCurve:=plot(ApFit,s=-Pi/2..5*Pi/2, color=blue, scaling=
constrained):
>display ({Points,FitCurve});

```

This curve specifies the aperture at the chosen value $t = 18\pi$.

To find the expression for $P(s)$, note that this aperture is $A(t) \times P(s) = a_0 e^{k_a 18\pi} P(s)$, so we need to divide by $a_0 e^{k_a 18\pi}$ to solve for the aperture shape function P .

```

>a:=t-> a0*exp(Ka*t);
>P:=ApFit/a(18*Pi);

```

The procedure “Shell” with the growth parameters determined above and the aperture curve P now produces a refined model:

```

>Shell(r0,z0,a0, Kr,Kz,Ka, P, 0,20*Pi, 500,50, 60,0, 1,1,1,
0.98,0.9,0.8, -90,-80, patchnograd):
>S[1];
>S[3];

```

Spiral ribs can be added to the model by incorporating an oscillatory function:

```

>P:=(ApFit/(a(18*Pi)))*(0.95+0.025*exp(sin(30*s)));
>Shell(r0,z0,a0, Kr,Kz,Ka, P, 0,20*Pi, 1000,100, 60,0, 1,1,1,
0.98,0.9,0.8, -80, -90, patchnograd):
>S[1];

```

Axial ribs or ridges are created by allowing the aperture shape to vary with t . Conceptually this replaces $P(s)$ by $P(s) \times Q(t)$. Equivalently, one can replace the constant a_0 by $a_0 Q(t)$ in the input to the Shell procedure.

```

>Shell(r0,z0, a0*(0.95+0.006*exp((exp(sin(30*t))))), Kr,Kz,Ka, P
, 0,20*Pi, 1000,100, 60,0, 1,1,1, 0.98,0.9,0.8, -80, -90,
patchnograd):
>S[1];

```

We sometimes plot a section of smooth “inner shell” at the body whorl together with the outer shell to give a more realistic image, one that reflects the different color and texture of the inside of the shell.

```

>Shell(r0,z0, a0*(0.95+0.006*exp((exp(sin(30*t))))), Kr,Kz,Ka, P
, 0,20*Pi, 1000,100, 60,0, 1,1,1, 0.98,0.9,0.8, -80, -90,
patchnograd):
>A:=S[1]:
>P:=ApFit/a(18*Pi):
>Shell(r0,z0, a0-0.02, Kr,Kz,Ka, P, 19*Pi,20*Pi, 50,100, 60,0,
1, 1, 1, 0.58,0.50,0.4, -80, -90, patchnograd):

```



```
>B:=S[1]:
>display({A,B});
```

6.3 Generating the color plate shells

Parameter values and aperture functions for the twelve seashell models shown in the color plates are given below. Appending these Maple commands to the Maple 12 procedure “Shell” in Section 6.1 generates each of the color plates.

Note: In Maple 12, right clicking on a graph gives a “glossiness” option, which we used to enhance a few of these images. For a couple shells, we have also plotted a contrasting “inner shell” to more closely mimic nature and to clarify the image at the body whorl.

Plate 1. Basic model of *E. magnificum* using circular apertures. Parameters are determined from measurements; see worksheet in Section 6.2.

```
> Shell(r0,z0,a0, Kr,Kz,Ka, 1, 0,20*Pi, 500,50, 60,0, 1,1,1,
0.98,0.9,0.8, -90, -80, patchnograd):
```

Plate 2. Refined model of *E. magnificum* incorporating Fourier aperture and surface ornamentation. Shell interior plotted separately in solid color for the body whorl and displayed together with exterior.

```
> Shell(r0,z0, a0*(0.95+0.006*exp((exp(sin(30*t))))), Kr,Kz,Ka,
P, 0,20*Pi, 1000,100, 60,0, 1,1,1, 0.98,0.9,0.8, -80, -90,
patchnograd):
> A:=S[1]:
> P:=ApFit/a(18*Pi):
> Shell(r0,z0, a0-0.02, Kr,Kz,Ka, P, 19*Pi,20*Pi, 50,100, 60,0,
1, 1, 1, 0.58,0.50,0.4, -80, -90, patchnograd):
> B:=S[1]:
> display({A,B});
```

Plate 3. Photograph of *E. magnificum* from Crow[2009].

Plate 4. Shell with spiral ribs; same growth parameters as Plate 8. Body whorl interior plotted separately.

```
> Shell(0.5, 1.7, 0.75*(1-0.05*(exp(sin(15*s))))), 0.15, 0.15,
0.15, 1, 0, 8*Pi, 300, 90, 60, 0, 0.75,0.75, 1, (1-0.18*(
exp(sin(15*s))))), 0.8 + 0.2*sin(5*s), 1, -116, -90,
patchnograd):
> A:=S[1]:
> Shell(0.5, 1.7, 0.65*(1-0.015*(exp(sin(15*s))))), 0.15, 0.15,
0.15, 1, 7*Pi, 8*Pi, 100, 90, 60, 0, 0.75, 0.75, 1, 0.95,
0.93, 0.94, -116, -90, patchnograd):
> B:=S[1]:
> display({A,B});
```

Plate 5. Cockle shell: $z_0 = k_z = 0$.

```
> Shell(0.001, 0, 0.5, 1, 0, 1.3, ((1-cos(s))-0.1*(exp(-(3*(s-Pi)
)/Pi)^2+(sin(20*(3*(s-Pi)/Pi)))^2))/1), 0, Pi, 400, 200, 20,
-45, 1,1,1, 0.8+0.2*(1-(t/(2*Pi))^(16)), 0.7+0.3*cos(120*(s
/(2*Pi))),0.8+0.2*sin(300*t/(2*Pi)), -133, -43, patchnograd):
```

Plate 6. Shell with axial ridges and non-circular aperture. Body whorl interior plotted separately.

```
> P:=s->piecewise(s<=Pi, min({2.5,abs((sec((s+Pi/8))))^(1/3)}),
Pi< s, 1);

> Shell(.5, 0.8, 0.35+0.005*exp(exp((cos(4*Pi*t)))), 0.15,
0.175, 0.175, P(s), 0, 6*Pi, 1200, 30, 60, 0, 0.75,0.75,1,
0.8+0.05*(cos(8*Pi*t)), 0.5, 0.5+0.5*((exp(cos(4*Pi*t))))),
-120, -100, patchnograd):

> A:=S[1]:
> Shell(.5, 0.8, 0.33, 0.15, 0.175, 0.175, P(s), 5*Pi, 6*Pi,
200, 30, 60, 0, 0.75,0.75,0.75, 0.3, 0.3, 0.6, -120, -100,
patchnograd):
> B:=S[1]:
> display({A,B});
```

Plate 7. Pointy-tipped shell: $k_r > k_z$.

```
>Shell(1,8, 2, 0.2, 0.12, 0.155, 1, 0, 8*Pi, 500, 40, 60, 0,
1,1,1, 0.7+ 0.3*(cos(2*t))^2, 0.7+0.3*(sin(2*s))^2, 0.8,
-116, -90, patchnograd):
```

Plate 8. Shell with linear helix envelope: $k_r = k_z$. Shell silhouette is also linear since $k_a = k_r = k_z$.

```
> Shell(0.5, 1.7, 0.75, 0.15, 0.15, 0.15, 1, 0, 8*Pi, 500, 50,
60, 0, 0.75,0.75,1, (sin(5*(s+sin(2*(t*s))))), 0.9, 1, -116,
-90, patchnograd):
```

Plate 9. Flat-topped shell: $k_r < k_z$.

```
> Shell(1, 1, 2, 0.175, 0.2, 0.16, 1, 0, 8*Pi, 500, 40, 60, 0,
0.75,0.75,1, 0.7+0.3*sin(10*s), 0.5+0.5*cos(10*t)*sin(10*s),
0.3+0.7*sin(10*t)*(cos(10*s)), -116, -90, patchnograd):
```

Plate 10. Loose spiral shell: $k_a < k_z$. Body whorl interior plotted separately.

```
> Shell(0.5, 1.7, 0.75, 0.15, 0.15, 0.12, 1, 0, 8*Pi, 500, 50,
60, 0, 1,0.75,1, 1-0.2*trunc(exp(sin(5*s))), 1-0.2*trunc(exp(
sin(3*s))), 1-0.2*trunc(exp(sin(2*s))), -116, -90,
patchnograd):
> A:=S[1]:
```

```

> Shell(0.5, 1.7, 0.7, 0.15, 0.15, 0.12, 1, 7.5*Pi, 8*Pi, 500,
50, 60, 0, 1,0.75,1, 0.5, 0.5, 0.5, -116, -90, patchnograd):
> B:=S[1]:
> display({A,B});

```

Plate 11. Clam shell: $z_0 = k_z = 0$.

```

> Shell(0.001, 0, 0.5, 1, 0, 1.3, 1-cos(s), 0, Pi, 100, 50, 20,
-45, 1,1,1, 1-(t/(Pi))^8, (1-(t/Pi)^8)*(1-cos(25*(s+Pi))),
(1-(t/Pi)^8)*(1-sin(50*(t+Pi))), -133, -43, patchnograd):

```

Plate 12. Body whorl engulfing previous ones: $k_a > k_z$. Body whorl interior plotted separately.

```

> Shell(0.5, 1.7, 0.75, 0.15, 0.15, 0.175, 1, 0, 8*Pi, 500, 50,
60, 0, 1,0.75,0.5, 0.7+ 0.2*(cos(t))^2 -0.4*sin(20*s),
0.8+0.2*(sin(2*s))^2 -0.4*sin(20*s), 0.7-0.4*sin(20*s), -116,
-90, patchnograd):
> A:=S[1]:
> Shell(0.5, 1.7, 0.71, 0.15, 0.15, 0.175, 1, 7*Pi, 8*Pi, 500,
50, 60, 0, 1,0.75,0.5, 0.98, 0.9, 0.9, -116, -90, patchnograd
):
> B:=S[1]:
> display({A,B});

```

Acknowledgement

We thank Stephen Crow for sharing his wonderful shell images and X-rays with us.

7 References and Sources

7.1 Print shell modeling resources

Adam, John. 2003. Mathematics in nature: modeling patterns in the natural world. Princeton, NJ: Princeton University Press. This text is a general resource for applied mathematics and mathematical modeling.

Bizikov, V.A. 2004. Shell in Vampyropoda (Cephalopoda): morphology, functional role & evolution (Ruthenica Supplement). Moscow: KMK Scientific Press. This journal supplement provides shell comparative functional morphology and microstructure.

Cortie, Michael. 1989. Models for mollusc shell shape. South African Journal of Science, 85: 454-460.

Cortie, Michael. 1993. Digital seashells. Computer & Graphics. 17, (1): 79-84. These articles review progress in shell models and describe ways to generate synthetic shells.

Dawkins, Richard. 1996. *Climbing mount improbable*. New York: W. W. Norton & Company. This popular science book discusses probability and its applications to evolution.

Flower, Rousseau H. 1964. *Nautiloid shell morphology*. New Mexico Institute of Mining and Technology, Bureau of Mines and Mineral Resources Memoir: Socorro. This foundational work focuses on external shell morphology and thin sections.

Fowler, Deborah, Hans Meinhardt, Przemyslaw Prusinkiewicz. 1992. Modeling seashells. *Proceeding of SIGGRAPH '92* (Chicago, Illinois, July 26-31), In *Computer Graphics*, 26, (2): 379-387. ACM SIGGRAPH, New York. This article offers shell modeling analysis similar to Chapter 10 of [Meinhardt, 2003].

Galbraith, Callum, Przemyslaw Prusinkiewicz, and Brian Wyvill. 2002. Modeling a *Murex cabritii* sea shell with a structured implicit surface modeler. *The Visual Computer*, 18: 70-80. This article gives a modeler to help capture shell surface perturbations and shell wall thickness.

Illert, Chris and Ruggero Santilli. 1995. *Foundations of theoretical conchology*. 2nd ed. Florida: Hadronic Press. This text argues that shells require a structurally general geometry.

Mandelbrot, Benoit. 1982. *The fractal geometry of nature*. New York: W. H. Freeman and Co. This text offers a definitive overview of fractal geometry and its applications.

McGhee, George, Jr. 1999. *Theoretical morphology: the concept and its applications* (The critical moments and perspectives in Earth history and paleobiology). New York: Columbia University Press. This text offers an overview of theoretical morphology and its future challenges.

Meinhardt, Hans. 2003. *The algorithmic beauty of sea shells*, 3rd ed. New York: Springer-Verlag. This book gives a rigorous study of modeling and computer simulations of seashell patterns.

Meinhardt, Hans and Martin Klinger. 1987. A model for pattern formation on the shells of molluscs. *Journal of Theoretical Biology*, 126: 63-89. This article offers models to generate mollusk shell pigmentation and relief-like patterns.

Oliver, Arthur P. H. and James Nicholls. 2004. *Guide to seashells of the world*. Buffalo, NY: Firefly Books. This is a comprehensive seashell identification resource.

Pickover, Clifford. 1989. A short recipe for seashell synthesis. *IEEE Computer Graphics and Applications* 9, (6): 8-11. This article provides artistic examples of seashell-like forms from a graphics supercomputer.

Prusinkiewicz, Przemyslaw and Deborah R. Fowler. 2003. Shell models in three dimensions. Chapter 10 of [Meinhardt 2003]. We significantly use this resource in our modeling approach in this module.

Raup, David. 1962. Computer as aid in describing form in gastropod shells. *Science*, 138: 150-152.

Raup, David. 1966. Geometrical analysis of shell coiling: general problems. *Journal of Paleontology*, 40, (5): 1178-1190.

Raup, David. 1969. Modeling and simulation of morphology by computer. In *Proceedings of the North American Paleontology Convention*, 71-83.

Raup, David and Arnold Michelson. 1965. Theoretical morphology of the coiled shell. *Science*, 147: 1294-1296. Raup's articles analyze shell morphology and computer-aided shell modeling.

Rupert, Edward and Robert Barnes. 1994. *Invertebrate zoology*. 6th ed. Fort Worth: Saunders College Publishing/Harcourt Brace Publishing. This introductory invertebrate biology text emphasizes adaptive morphology and physiology.

Stone, Jon R. 1995. CerioShell; a computer program designed to simulate variation in shell form. *Paleobiology*, 21: 509-519.

Stone, Jon R. 1996. The evolution of ideas: a phylogeny of shell models. *The American Naturalist*, 148: 904-929.

Stone, Jon R. 1997. The spirit of D'Arcy Thompson dwells in empirical morphospace. *Mathematical Biosciences*, 142: 13-30. Stone's articles describe shell model evolution and recent connections to classic approaches.

Thompson, D'Arcy. 1961. *On Growth and Form*. Great Britain: University Press, Cambridge. This work explores form and structure in living organisms from a mathematical perspective.

Wilbur, Karl, E.R. Trueman, and M.R. Clarke (Eds.). 1988. *The mollusca: form and function*, Volume 11. San Diego, CA: Academic Press. This text reviews advances in interpreting the structure and function of mollusk systems.

7.2 Online shell modeling resources

American Mathematical Society. 2004. The mathematical study of mollusk shells. Available at: <http://www.ams.org/featurecolumn/archive/shell1.html>, accessed 27, January, 2009. This column describes how logarithmic spirals can help develop mollusk shell geometry.

Coombes, Stephen. 2000. The geometry of sea shells. Available at: <http://www.maths.nott.ac.uk/personal/sc/SeaShells.pdf>, accessed 27, January, 2009. This University of Nottingham document offers mathematical background for shell models.

Duke University. 1997-2003. "Connected Curriculum Project." Available at: <http://www.math.duke.edu/education/ccp/materials/biology.html>, accessed 27, January, 2009. This site offers two modules that create equiangular spirals using a CAS.

Ferraro, Roberto. 2000. LS sketchbook by example: Sea shells and horns. Available at:

<http://coco.ccu.uniovi.es/malva/sketchbook/lssketchbook/examples/seashell/seashell.htm>, accessed 27, January, 2009. This page presents some software/code for sketching spirals and shell models.

International Educational Software. 2003. Snail shell Manipula Math with Java. Available at <http://www.ies.co.jp/math/java/misc/oum/oum.html>, accessed 27, January, 2009. This site provides a java applet for creating a snail shell according to a log clock model.

Jirapong, Kamon, Robert J. Krawczyk. 2003. Seashell architectures. Paper given at ISAMA/Bridges Conference. Available at: <http://www.iit.edu/~krawczyk/kjbrdg03.pdf>, accessed 27, January, 2009. This site describes a study to apply seashell form to architecture.

Kazlev, M. Alan. 2002. Palaeos invertebrates: Mollusca: Mollusc shell morphology." Available at: <http://www.palaeos.com/Invertebrates/Molluscs/Mollusca.Shell.html>, accessed 27, January, 2009. This site offers information on mollusk shell modeling and Raup's models from the 1960s.

Lee, Xah. 1995-2008. Mathematics of seashell shapes. and Equiangular spiral. Available at: http://xahlee.org/SpecialPlaneCurves_dir/Seashell_dir/index.html, accessed 27, January, 2009. These pages provide information and some CAS/graphing calculator code to model seashells.

Lucca, G. 2003. Representing seashells surface. Visual Mathematics. 5: 1. Available at <http://www.mi.sanu.ac.yu/vismath/lucca/>, accessed 27, January, 2009. This paper presents a general algorithm to model various seashell shapes and some examples.

Moidel, Chuck. Sea shells. WPI. Available at: http://www.cs.wpi.edu/~emmanuel/courses/cs563/write_ups/chuckm/seashells.htm, accessed 27, January, 2009. This article offers information on shell modeling, pigmentation, and relevant biochemistry.

Peterson, Ivars. 2005. Sea shell spirals. Science News. Available at: http://www.sciencenews.org/view/generic/id/6030/title/Math_Trek__Sea_Shell_Spirals, accessed 27, January, 2009. This column argues that nautilus shell growth is not based on a golden ratio equiangular spiral.

Phillips, Tony. 2001. The mathematical study of mollusk shells. Available at: <http://www.math.sunysb.edu/~tony/whatsnew/column/shells-0201/shell1.html>, accessed 27, January, 2009. This column describes how equiangular spirals can generate mollusk shell geometry.

Picado, Jorge. 2009. Seashells: the plainness and beauty of their mathematical description. Loci (the online digital magazine of the MathDL). Available at <http://mathdl.maa.org/mathDL/23/?pa=content&sa=viewDocument&nodeId=3294>, accessed 19, May 2009. This article includes a simple model to describe and generate many types of seashell shapes.

TONMO.com. 2000-2009. The octopus news magazine online. Available at: <http://www.tonmo.com/science/fossils/morphology/>, accessed 27, January, 2009. This site

offers a variety of shell morphology information.

Wang, Ngai-Ming. 1997. Modeling seashells in OpenGL. Cornell University. Available at: <http://www.nbb.cornell.edu/neurobio/land/OldStudentProjects/cs490-96to97/wang/re2.html>, accessed 27, January, 2009. The author models various seashells by sweeping a curve along a helico spiral in Open GL.

7.3 Online sources for shells, pictures, and X-rays

American Malacological Society homepage. 2009. Available at: <http://www.malacological.org/>, accessed 27, January, 2009. The AMS is an international society interested in the conservation and study of mollusks.

Beechey, Des. The sea shells of New South Wales. Available at: <http://seashellsofnsw.org.au/>, accessed 27, January, 2009. This site offers information about various shell species and a handy shell glossary.

Bourquin, Avril. 2009. Man and Mollusc/Mollusk. Available at: <http://manandmollusc.net/>, accessed 27, January, 2009. This comprehensive site provides various shell articles and a handy Internet resource zone.

Conchking store homepage. 2009. Available at: <http://conchking.com/Seashells.htm>, accessed 27, January, 2009. This online store offers a wide range of Caribbean seashells.

Conch-Net or Conchologists Information Network homepage. 1996-2009. Available at: <http://www.conchologistsofamerica.org/home/>, accessed 27, January, 2009. This site provides American Conchologist shell articles and other relevant information.

Crowncity seashell posters. 2009. Available at: <http://www.crowncity.com/shellfish/>, accessed 27, January, 2009. This page offers shell printer made using an X-ray machine.

Crow, Stephen. 2009. Seashell architecture. Available at: <http://www.seashellarchitecture.com/>, accessed 27, January, 2009. Offering a large collection of seashell X-rays, this site is the source of the CD for our X-rays.

Cummings, Kevin, Anton Oleinik, and John Slapcinsky. 2008. Systemic research collections.” Available at: http://www.inhs.uiuc.edu/cbd/main/collections/mollusk_links/museumlist.html, accessed 27, January, 2009. This page details research collections of recent and fossil mollusks from around the world.

Egerton, Peter. 2000. Peters sea shells homepage. Available at: <http://www.petersseashells.ca/shellcore.html>, accessed 27, January, 2009. This site offers morphology and seashell information and a useful page with pertinent links.

University of California Museum of Paleontology. 2001. Mollia homepage. Available at: <http://www.ucmp.berkeley.edu/mologis/mollia.html>, accessed 27, January, 2009. This site offers information about various malacological journals, a listserve, and newsletter.

Poppe, Guido and Philippe Poppe. 1996-2009. Conchology, Inc. Available at <http://www.conchology.be/en/home/home.php>, accessed 27, January, 2009. This site presents for sale thousands of shell photographs.

Power, Emilio. The macalogical cabinet. 2005. Available at: <http://pw1.netcom.com/~ejpower/macab/malcabinet.htm>, accessed 27, January, 2009. This site displays some rare mollusks and links to other informational/education sites.

Schultz, Randolf. 2008. The shelly lib homepage. Available at: <http://www.shelly.de/sl.html>, accessed 27, January, 2009. This is a small library with applications to create shapes and textures of seashells and snails.

Worldwide Conchology. 2009. Conchology: The art and science of nature. Available at: <http://www.worldwideconchology.com/MainFrames.shtml>, accessed 27, January, 2009. This site offers a family index for mollusks and high quality digital images of various shells.

Biographies



George Ashline received his B.S. from Saint Lawrence University, his M.S. from the University of Notre Dame, and his Ph.D. from the University of Notre Dame in complex analysis. He has taught at Saint Michael's College for many years. He is a participant and consultant in Project NExT, a program created for new or recent Ph.D.s in the mathematical sciences. He is also actively involved in mathematics professional development programs for elementary and middle level educators.



Joanna Ellis-Monaghan received a B.A. in visual arts and mathematics from Bennington College, an M.S. in mathematics from the University, and a Ph.D. from the University of North Carolina at Chapel Hill in 1995 in algebraic combinatorics. Her current research areas are algebraic combinatorics and applied graph theory, with an emphasis on bioinformatics and statistical mechanics. She is a proponent of active learning and has developed a broad range of classroom materials, much of it technology-based, to augment a variety of courses. She is also involved in undergraduate student research, is a Project NeXT consultant, and is on the Maple Academic Advisory Board.



Zsuzsanna Kadas received her B.S. in Mathematics and Physics from St. John's University (1974) and her M.S. and Ph.D. in Applied Mathematics from Rutgers University (1982). She taught at the University of Vermont and has been Professor of Mathematics at Saint Michael's College for many years. Her specialty is differential equations and mathematical models in biology, and she especially enjoys teaching students about the power of mathematics to describe nature and the physical world.



Declan McCabe earned his B.S. in Biology at St. Joseph's University in Philadelphia, M.S. in Ecology and Evolution at the University of Pittsburgh, and his Ph.D. in Ecology from the University of Vermont. He teaches introductory and upper-level courses in the Biology Department at Saint Michael's College. As a science advisor for the Vermont EPSCoR streams project (<http://www.uvm.edu/~streams/>), he has combined research and outreach in a program that involves high school and undergraduate students in ecological research. Teaching materials developed by future primary school teachers in his Biology in Elementary Schools course are at: http://www.wikieducator.org/Biology_in_elementary_schools.